Progress on Ultra-Heavy Cosmic-Ray Analysis with CALET on the International Space Station

Wolfgang V. Zober[a], Brian F. Rauch[a], Anthony W. Ficklin[b] and Nicholas Cannady [c] on behalf of the CALET Collaboration
[a]Department of Physics and McDonnell Center for the Space Sciences, Washington University, St. Louis, MO 63130 USA
[b]Department of Physics and Astronomy, Louisiana State University, Baton Rouge, LA 70803 USA
[c]CRESST-II/University of Maryland, Baltimore County/NASA Goddard Space Flight Center

Abstract

CALET, the Calorimetric Electron Telescope, launched to the International Space Station in August 2015 and in continuous operation since, has gathered over seven years of data so far. CALET is able to measure cosmic-ray (CR) electrons, nuclei, and gamma rays and with its 27 radiation length deep Total Absorption Calorimeter (TASC), measures particle energy, allowing for the determination of spectra and secondary to primary ratios of the more abundant CR nuclei through $_{28}$Ni, while the main charge detector (CHD) can measure Ultra-Heavy (UH) CR nuclei through $_{40}$Zr. CALET UHCR analyses use a special high duty cycle UH trigger with an expanded geometry that does not require passage through the TASC. To effectively analyze UHCR trigger events, a number of screens and corrections have been developed for the analysis. From time- and position-dependent detector response corrections based on $_{14}$Si and $_{26}$Fe, to an angle-dependent geomagnetic cutoff rigidity selections and minimum deposited energy screens, a number of methods have been explored to optimize UH statistics to varying effect. In this work, we aim to show how these event selection screens and corrections have been developed, how the rigidity screens shown previously by Rauch et al compare to the newer TASC methodology shown in our other ICRC paper, and how TASC selections may be used to influence analysis on the full UH-trigger dataset.

CALET Instrument

The main science objective of CALET is to directly measure the total cosmic-ray electron flux (e^-+e^+) to the highest energies (1 GeV to 20 TeV) with the main calorimeter (CAL), shown in the CALET instrument package in Fig. 1a. The calorimeter is also capable of measuring gamma rays (10 GeV to 10 TeV) and cosmic-ray nuclei (up to 1,000 TeV) [**?**].
The instrument is comprised of three detector systems: (Fig. 1b)

- The charge detector (CHD), comprised of an x and y layer with 14 scintillator paddles. Each paddle is 32 mm wide by 10 mm thick by 450 mm long. Provides the primary particle charge identification.
- Below that layer is the imaging calorimeter (IMC), which is 156.5 mm tall and made of 8 layers of x and y scintillating fibers that are 1 mm square and 448 mm long. Utilized for track reconstruction
- The total absorption calorimeter (TASC). This is made of 6 x and y layers of 16 lead tungstate (PWO) scintillator logs which gives a determination of particle energy.

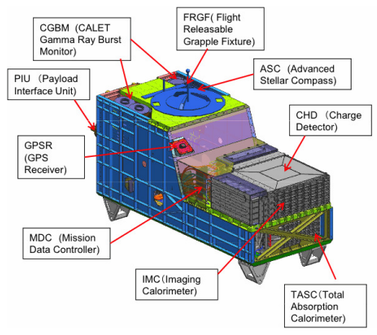

Figure 1(a): CALET instrument package detailing location of various CALET subsystems.

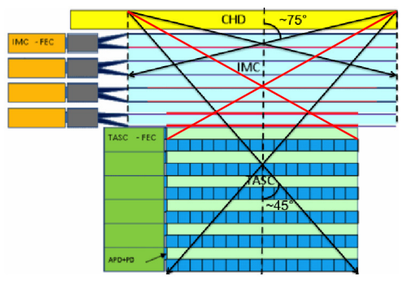

Figure 1(b): CALET side-view showing CHD, IMC, and TASC detector placement with the maximum acceptance angles for detection. In the UH trigger analysis this is 75° and in the TASC analysis this is 45°.

Position Corrections

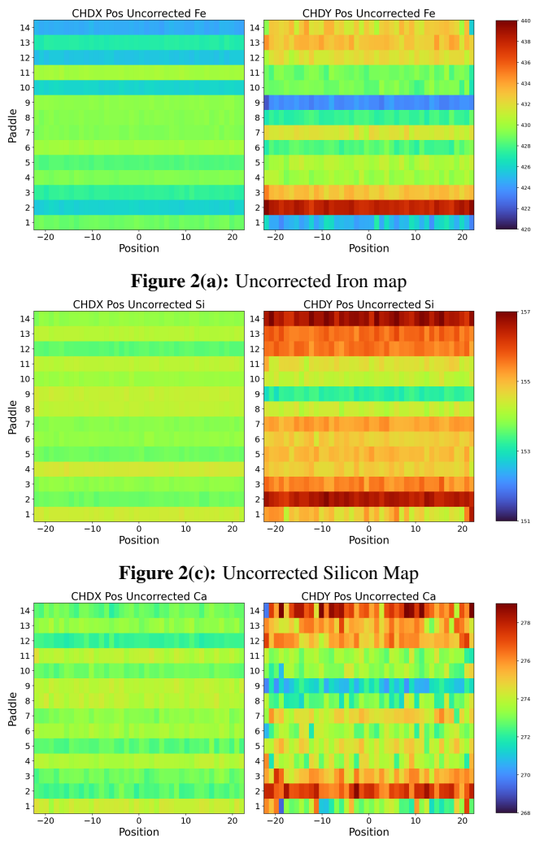

Figure 2(a): Uncorrected Iron map

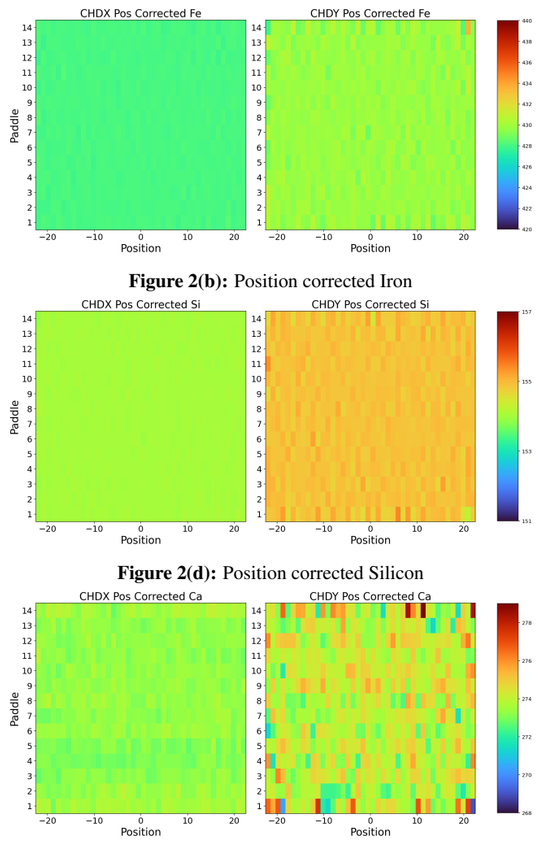

Figure 2(b): Position corrected Iron

Figure 2(c): Uncorrected Silicon Map

Figure 2(d): Position corrected Silicon

Figure 2(e): Uncorrected Calcium map

Figure 2(f): Calcium map post-correction

The position corrections are derived by dividing each CHD paddle into 42 segments (with length $\sim$ 1/3 of paddle width). For each individual paddle segments we perform a Gaussian fit on $_{26}$Fe and $_{14}$Si events to determine the local mean energy for those elements. We then take these local means and find the ratio of the full layer means for both $_{26}$Fe and $_{14}$Si respectively. We then plug these ratios into a scaling function with a hyperbolic tangent function to allow for proportional scaling for elements between $_{14}$Si and $_{26}$Fe and single correction factor domination outside that range. This allows a smooth transition across all CHD signal. The equation shown in Eqn. 1 defines $S(x)$ as the initial signal of an event, Si_{ratio} and Fe_{ratio} as the correction ratios for

$$S(x)_{corr} = S(x)Si_{ratio} + \left[1 + \tanh\left(\frac{1}{40}\left(S(x) - \frac{Si_{avg} + Fe_{avg}}{2}\right)\right)\right]\frac{S(x)Fe_{ratio} - S(x)Si_{ratio}}{2} \quad (1)$$

that event location and Si_{avg} and Fe_{avg} are the full layer means.

Acknowledgments

We gratefully acknowledge JAXA's contributions to the development of CALET and to the operations onboard the International Space Station. We also express our sincere gratitude to ASI and NASA for their support of the CALET project. This work was supported in part by JSPS Grant-in-Aid for Scientific Research (S) Grant No. 19H05608. The CALET effort in Italy is supported by ASI under Agreement No. 2013- 018-R.0 and its amendments. The CALET effort in the U.S. is supported by NASA through Grants No. 80NSSC20K0397, No. 80NSSC20K0399, and Np. NNH18ZDA001N-APRA18-004, and under award Np. 80GSFC21M0002.
The material contained in this document is based upon work supported by a National Aeronautics and Space Administration (NASA) grant or cooperative agreement. Any opinions, findings, conclusions, or recommendations expressed in this material are those of the author and do not necessarily reflect the views of NASA.

References

[1] S. Torii for the CALET Collaboration, *Highlights from the CALET observations for 7.5 years on the International Space Station*, in proceedings of *The 38th International Cosmic Ray Conference*, (2023)
[2] O. Adriani et al. (CALET Collaboration), *Measurement of the Iron Spectrum in Cosmic Rays from 10 GeV/n to 2.0 TeV/n with the Calorimetric Electron Telescope on the International Space Station* Phys. Rev. Lett. 126, 241101, 2021
[3] O. Adriani et al. (CALET Collaboration), *Direct Measurement of the Nickel Spectrum in Cosmic Rays in the Energy Range from 8.8 GeV/n to 240GeV/n with CALET on the International Space Station* Phys. Rev. Lett. 128, 131103, 2022
[4] G. Tarle, S. P. Ahlen, and B. G. Cartwright. *Cosmic Ray Isotope Abundances from Chromium to Nickel*. ApJ, 230(1979), 607–620.
[5] W.V. Zober et al. *Progress on Ultra-Heavy Cosmic-Ray Analysis with CALET on the International Space Station* in proceedings of *The 37th International Cosmic Ray Conference*, (2021)
[6] W.V. Zober and B.F Rauch for the CALET Collaboration, *Results of the Ultra-Heavy Cosmic-Ray Analysis with CALET on the International Space Station*, in proceedings of *The 38th International Cosmic Ray Conference*, (2023)

Time Corrections

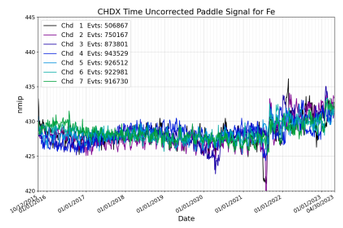

Figure 3(a): Uncorrected Iron signal for CHDX Paddles 1-7.

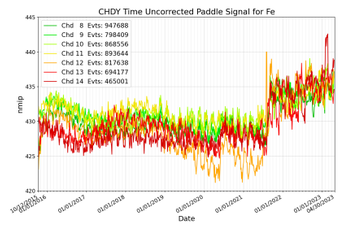

Figure 3(b): Uncorrected Iron Signal for CHDY for paddles 8-14.

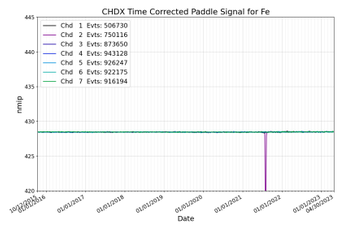

Figure 3(c): Time Corrected signal for CHDX Paddles 1-7.

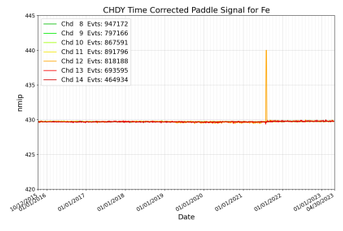

Figure 3(d): Time Corrected signal for CHDY Paddles 8-14
.

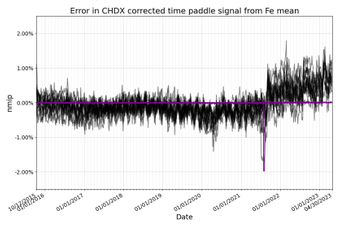

Figure 3(e): Overlay of pre- and post-time corrections for CHDX Iron. Black shows percent error for the full layer mean for Iron on CHDX. Purple shows percent error post correction.

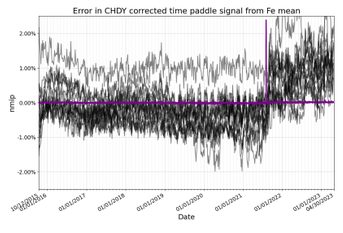

Figure 3(f): Overlay of pre- and post-time corrections for CHDX Iron. Black shows percent error for the full layer mean for Iron on CHDY. Purple shows percent error post correction.

The time corrections are performed similarly to the position corrections, with the "local" segments being defined as increments in time such that there are a minimum 550 $_{26}$Fe events in the final paddle of CHDY for each time step. This results in time correction bins being approximately 3 days in length.

Energy Corrections

We take an initial Tarle charge assignment [4] of CHDX and CHDY to determine the set of candidate $_{26}$Fe events, which is any event within 1-sigma of the $_{26}$Fe peak. From this we divide the full UH TASC subset into 65 energy bands, with each having $\sim$61000 $_{26}$Fe candidate events.
With these sets we iterate through the bins performing a multi-Gaussian peak fit on the CHDX (Figure 4a) and CHDY (Figure 4b) event histograms. These plots show an initial charge based on taking the square root of signal which would corresponds to a Tarle function with A=0 and C=1. From this we can take a multipeak Gaussian fit, initialized with randomized initial peak height to force peak searching routine to fully explore the parameter space and with bounds of $\pm$ 0.15 units on the psuedo-Z scaling. With the identified peak centers, we are able perform a Tarle model fit to find the actual coefficients of the model.

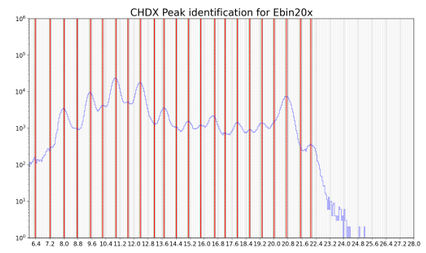

Figure 4(a): Peak identification for CHDX. Blue histogram denotes data, vertical red line denotes the fit routine's guess on peak center. Horizontal axis units are based on the square root of CHDX signal.

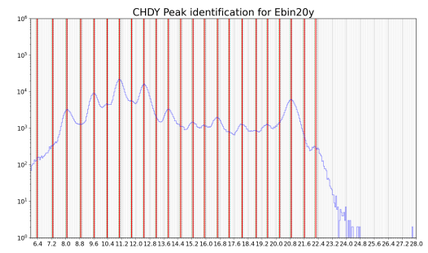

Figure 4(b): Peak identification for CHDY. Blue histogram denotes data, vertical red line denotes the fit routine's guess for peak center. Horizontal axis units are based on the square root of CHDY signal.

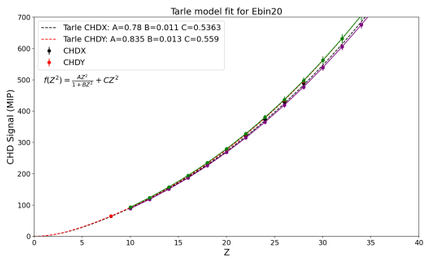

Figure 4(c): Fits to identified peaks in Figure 4a and 4b.

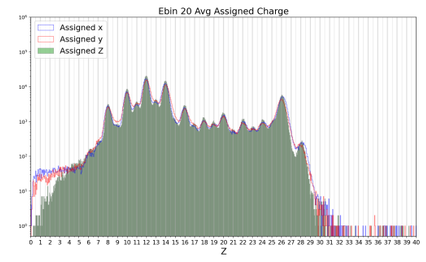

Figure 4(d): Red and blue histograms represent the CHDX and CHDY assigned Z. Green shaded region represents the final average of CHDX and CHDY.

Screen Selection

As shown in the main CALET UH proceeding [6], after all corrections are performed, we want to perform a small number of event selection screens. This is to remove lower quality events.
The first screen on the lowest three energy bins is not shown here, but was based on the results of the previous energy based Tarle charge assignment. The lowest three bins suffered from severe smearing of charge and prevented many peaks between $_{14}$Si and $_{26}$Fe from being identified. Since a clean charge assignment could not be done in those energy bands, we screen out those bins.

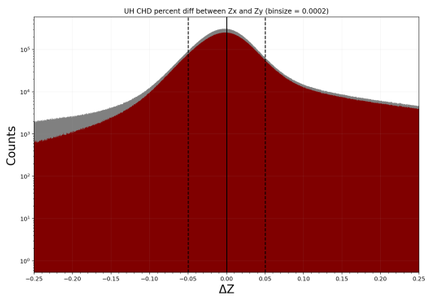

Figure 5(a): Histogram showing how events counts vary with percent difference in CHDX and CHDY. All events are in gray. The maroon histogram shows events with Edep $\geq$ 1.535 nmip and not on CHD edge. Binned in 0.02% increments.

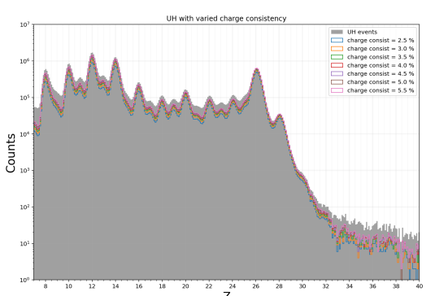

Figure 5(b): Histogram showing how changes in maximum percent difference in charge consistency change relative peak height and peak shape.

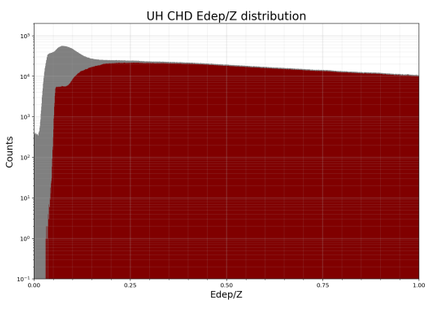

Figure 5(c): Histogram showing how event counts vary with Edep/Z. All events in gray. Maroon histogram shows events with Edep $\geq$ 1.535 nmip and not on CHD edge. Histogram has a fine binning resolution of 0.005 nmip/Z.

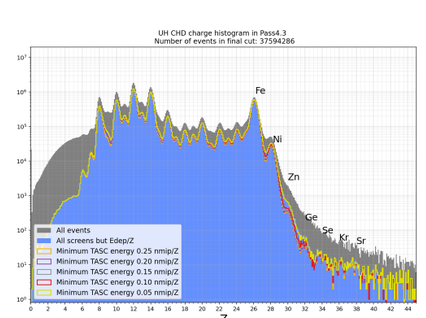

Figure 5(d): Histogram showing how changes in minimum deposited energy change the relative peak height and peak shape. Higher energies create clearer peaks at the cost of statistics.

Figure 5a and 5b show how minor changes in percent difference in CHDX and CHDY alter the final histogram. We see that the percent difference is not symmetric, so a good screen needs to occur at value below that asymmetry. The dashed lines added in Figure 5a at $\pm$ 0.05% highlight where the asymmetry in CHDX and CHDY approximately begins and constrain the maximum percent difference. Figure 5c and 5d show how Edep/Z behaves, we aim to be past the odd feature and curve, $\sim$0.15 nmip/Z.